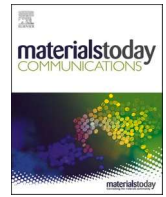


Contents lists available at ScienceDirect

Materials Today Communications

journal homepage: www.elsevier.com/locate/mtcomm

Nanoneedle-shaped zinc oxide enabled ultraflexible chemiresistive NO sensor

Yang Zhang^{a,e,1}, Yipeng Pang^{d,1}, Chunying Ou^a, Tao Zhang^b, Haiting Xu^b, Jing Xu^b,
Li Yang^{c,*}, Manhua Ding^{b,e,**}

^a Department of Neurology, Xuzhou Central Hospital, Southeast University Affiliated Xuzhou Central Hospital, Xuzhou Clinical School of Xuzhou Medical University, Xuzhou, China

^b Department of Radiotherapy, Xuzhou Cancer Hospital, Xuzhou, China

^c Jiangsu Province Key Laboratory of Anesthesiology, Xuzhou Medical University, Xuzhou, China

^d School of Life Sciences, Xuzhou Medical University, Xuzhou, China

^e Suzhou Medical College, Soochow University, Suzhou, China

ARTICLE INFO

Keywords:

Nitric oxide (NO) sensor
Needle-shaped
Zinc oxide (ZnO)
Ultraflexible

ABSTRACT

Inhalation of environmental nitric oxide (NO) has been implicated in neurological disorders such as stroke and glioma, underscoring the urgent need for sensitive, reliable NO detection in wearable biomedical diagnostics. However, achieving high sensitivity alongside mechanical durability and stability under continuous deformation remains challenging. Here, we report an ultraflexible chemoresistive NO sensor based on needle-shaped zinc oxide (ZnO) nanostructures, which deliver enhanced gas-sensing performance with exceptional mechanical resilience. The needle-like morphology offers a high surface-to-volume ratio for efficient gas adsorption, while abundant nanoscale junctions create multiple conductive pathways, maintaining stable electrical contact under extreme bending and prolonged stress. Compared to conventional dense ZnO films, our sensors exhibit superior performance, including high sensitivity ($S = 59.4$), rapid room-temperature NO detection (response time < 50 s), and excellent selectivity against common interfering gases. Such sensor operates stably in high humidity ($> 80\%$ RH), broadening its applicability. Critically, it endures bending radii as small as 1 mm and retains stable electrical output after 500 cycles. This synergistic combination of ultrasensitive detection, environmental tolerance, and mechanical robustness positions our ZnO-based platform as a promising candidate for real-time health monitoring and environmental sensing, with particular relevance to NO-associated neurological diseases.

1. Introduction

Nitric oxide (NO) is a crucial signaling molecule in biological systems, playing a pivotal role in clinical medicine due to its significance in the diagnosis and management of various diseases. As a key endothelial-derived mediator, NO regulates vascular dilation and constriction, thereby maintaining blood pressure homeostasis and ensuring adequate blood flow [1–3]. Dysregulation of NO levels is closely associated with cardiovascular diseases such as hypertension, atherosclerosis, stroke, gliomas, and cerebral infarction [4–7]. Notably, excessive NO production can induce neuronal apoptosis and necrosis, contributing to neurotoxicity. Consequently, precise NO detection is essential for

accurate diagnosis and the development of targeted therapeutic strategies [8]. Beyond its physiological roles, NO is also a major environmental pollutant, primarily emitted through fossil fuel combustion from transportation and industrial activities [9]. In the atmosphere, NO rapidly oxidizes to nitrogen dioxide (NO_2), a precursor to secondary air pollutants such as ozone and fine particulate matter ($\text{PM}_{2.5}$), which pose severe threats to human health and ecological stability. Prolonged exposure to elevated NO_2 levels exacerbates respiratory diseases, impairs lung function, and increases the risk of cardiovascular disorders [10–12]. Additionally, NO contributes to acid rain formation, leading to soil and water acidification and endangering biodiversity [13,14]. Therefore, accurate NO monitoring is critical not only for advancing

* Corresponding author.

** Corresponding author at: Department of Radiotherapy, Xuzhou Cancer Hospital, Xuzhou, China.

E-mail addresses: yangli2021@xzhmu.edu.cn (L. Yang), dingmanhuab@126.com (M. Ding).

¹ These authors contributed equally to this work.

clinical diagnostics and disease management but also for mitigating air pollution and its detrimental impacts on public health and ecosystems.

Detection methods for NO have undergone significant advancement over the past few decades, encompassing techniques such as chemiluminescence, spectroscopy, electrochemistry, and gas chromatography [15–21]. Each of these conventional methods presents distinct advantages and limitations. Chemiluminescence, for instance, offers high sensitivity and selectivity; however, it is hindered by high equipment costs and operational complexity [15]. Spectrometry facilitates real-time monitoring but demands stringent environmental conditions and often requires costly laser sources [22–24]. Although electrochemical methods are relatively straightforward and cost-effective, their selectivity and stability can deteriorate over extended periods, making them vulnerable to environmental variations. Gas chromatography provides high-resolution analysis; nevertheless, its large apparatus and cumbersome operation can limit field applications. Thus, flexible resistive NO sensors emerge as a promising alternative [19]. Firstly, flexible sensors exhibit excellent adaptability, enabling their application on various complex and irregular surfaces, which is particularly advantageous for wearable devices and smart electronics. Furthermore, these sensors typically feature low fabrication costs and straightforward production processes, facilitating mass production and thereby reducing barriers to market entry. By optimizing material properties and structural design, these sensors can detect NO fluctuations within brief timeframes, fulfilling the demands of real-time monitoring [25–29]. Additionally, their enhanced conductivity and tunable sensitivity allow for adjustments based on different detection environments, thereby improving accuracy. Lastly, flexible resistive NO sensors possess substantial potential for both environmental monitoring and clinical applications [30–32]. In environmental contexts, they can be deployed for real-time urban air quality assessments, providing valuable data to inform policy decisions. In clinical settings, these sensors can facilitate the detection of respiratory gases, aiding in the early diagnosis and ongoing monitoring of respiratory diseases [33,34]. Therefore, the advent of flexible resistive NO sensors addresses these shortcomings, advancing NO detection technology to meet the increasing demands of various markets.

In this work, we developed an ultraflexible chemoresistive NO sensor based on needle-shaped zinc oxide (ZnO) nanostructures, demonstrating superior performance over conventional dense ZnO film. By leveraging the unique morphology of ZnO nanoneedles, which provide an extensive surface area for gas adsorption and multiple conductive pathways for charge transport, the sensor exhibits outstanding NO detection capabilities, including high sensitivity, rapid response and recovery times, excellent selectivity, and remarkable resistance to high-humidity environments. Beyond its exceptional gas-sensing performance, the needle-shaped ZnO sensor exhibits extraordinary mechanical robustness. Systematic bending tests confirmed its ability to maintain stable electrical operation under extreme mechanical deformation, even at ultra-small bending radii and after prolonged cyclic bending. Unlike dense ZnO films, which suffer from crack formation and conductive pathway disruption under mechanical stress, the nanoneedle architecture effectively mitigates stress concentration through structural adaptability, including inter-nanoneedle sliding and realignment, thereby ensuring long-term durability and sustained sensing performance. This work lays a solid foundation for the future development of flexible and wearable gas sensors, paving the way for innovative applications in personalized healthcare, smart environmental monitoring, and next-generation electronic skin systems.

2. Experimental section

2.1. Materials and chemicals

ZnO was purchased from Merck, while needle-like ZnO was obtained from WOW Materials. The photoresist AZ4620 and the developer

AZ400K, used for photolithography, were sourced from Micro-Chemicals. Solvents such as acetone, isopropanol, and ethanol were purchased from Sigma.

2.2. Device fabrication

To fabricate an ultraflexible substrate, a Micro-90 sacrificial layer is first spin-coated onto a cleaned substrate, followed by the deposition of a 3 μm -thick parylene layer. Gold electrodes are then patterned via photolithography: AZ4620 photoresist is spin-coated at 3000 rpm to achieve the desired thickness, soft-baked at 110°C for 2 min to remove residual solvents, and exposed to 365 nm UV light through a photomask with an exposure dose of $\sim 250 \text{ mJ}/\text{cm}^2$. The exposed resist is developed in a diluted AZ400K solution (AZ400K:H₂O = 1:3) for 1 min, rinsed with deionized (DI) water, and dried with nitrogen. A Cr/Au (5/50 nm) bilayer is deposited via electron beam evaporation, where Cr enhances adhesion and Au serves as the conductive electrode. Lift-off is performed by immersing the sample in acetone, followed by nitrogen drying to yield the patterned electrodes. Finally, the ultraflexible substrate is released by dissolving the sacrificial layer in DI water.

2.3. Characterization

The surface morphology and elemental composition of both dense and needle-shaped ZnO were analyzed using a scanning electron microscope (Gemini SEM 300) equipped with energy-dispersive X-ray spectroscopy (EDS). The electrical characteristics of the NO sensors were systematically evaluated in a controlled environment using a semiconductor parameter analyzer (B1500A). Gas sensing measurements were performed within an airtight chamber ($\sim 0.01 \text{ L}$), where the sensors were exposed to test atmospheres generated by mixing dry air with predefined concentrations of NO and potential interfering gases, including ammonia (NH₃), carbon monoxide (CO), formaldehyde (HCHO), and ethanol. The gas mixture was introduced into the chamber at a constant flow rate of 100 standard cm³/min via a mass flow controller. Humidity conditions were precisely regulated by adjusting the mass flow ratios of dry air, humidified air (produced by bubbling through distilled water), and the target NO gas.

3. Results and discussion

3.1. Design principle of needle-shaped ZnO resistive sensor

Nitric oxide (NO), a critical gaseous signaling molecule, plays essential roles in regulating blood pressure and immune responses within the human body. However, excessive accumulation of NO can contribute to a range of health issues, including cardiovascular diseases, neurodegeneration, and pulmonary disorders (Fig. 1a). Additionally, NO emissions pose significant environmental risks, such as contributing to air pollution, stratospheric ozone depletion, and acid rain formation. Consequently, the development of efficient NO sensors is crucial for the real-time monitoring of NO concentrations in both biological and environmental contexts, enabling timely interventions to mitigate these potential health and environmental hazards. Based on this, we proposed a needle-shaped ZnO resistive sensor for monitoring of NO molecules, the principle of a such sensor for detecting NO is primarily governed by the interaction between NO molecules and the ZnO surface. Specifically, when NO interacts with the surface, it reacts with oxygen vacancies to form nitrogen-oxide intermediates, which in turn modulate the charge carrier density in the ZnO, affecting its electrical conductivity (Fig. 1b). Monitoring the changes in the sensor's resistance enables the quantitative detection of NO concentrations in the surrounding environment. The needle-shaped ZnO significantly increases the surface area, enhancing gas molecule adsorption and improving the sensor's response time and sensitivity (see below). As a result, resistance-based sensors utilizing needle-shaped ZnO would exhibit superior performance in NO

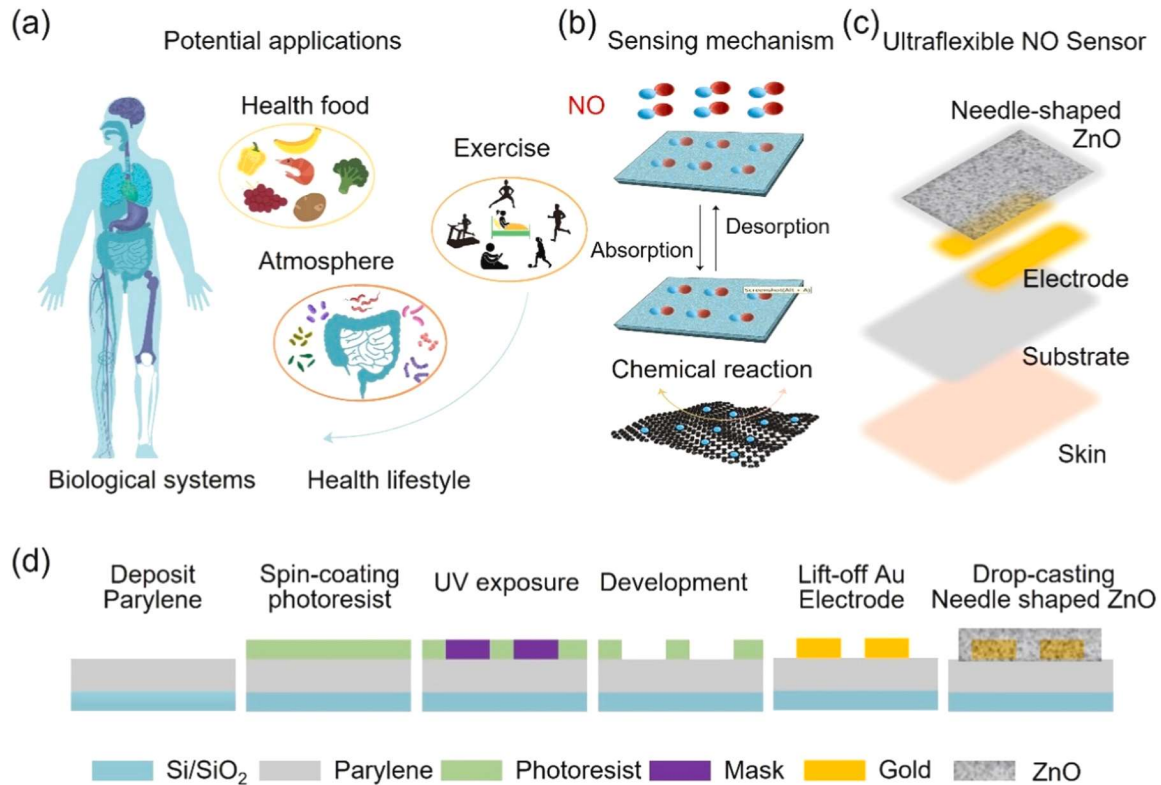


Fig. 1. Application scenarios, design principles, and fabrication process of the NO sensor. (a) Schematic illustration of the NO sensor design principles. (b) Mechanism of the NO sensor. (c) Device structure of the ultraflexible NO sensor. (d) Photolithographic fabrication process of the ultraflexible NO sensor.

gas detection. Device structure design can be illustrated in Fig. 1c, and this sensor consists of three parts: ultraflexible substrate, electrical signal transmission electrode and active substance of needle-shaped ZnO. The sensing devices were fabricated on an ultraflexible Parylene substrate using a standard photolithography process, as illustrated in Fig. 1d. The fabrication procedure consists of six key steps, detailed in the Methods section. This well-established photolithographic approach

ensures the uniformity and stability of the sensors, maintaining their reliable performance.

Next, scanning electron microscopy (SEM) was employed to investigate the microstructural characteristics of needle-like ZnO, indicating that ZnO nanoneedles typically form uniformly aligned structures, with diameters ranging from tens to several hundred nanometers and lengths extending up to a few micrometers (Fig. 2a). High-magnification SEM

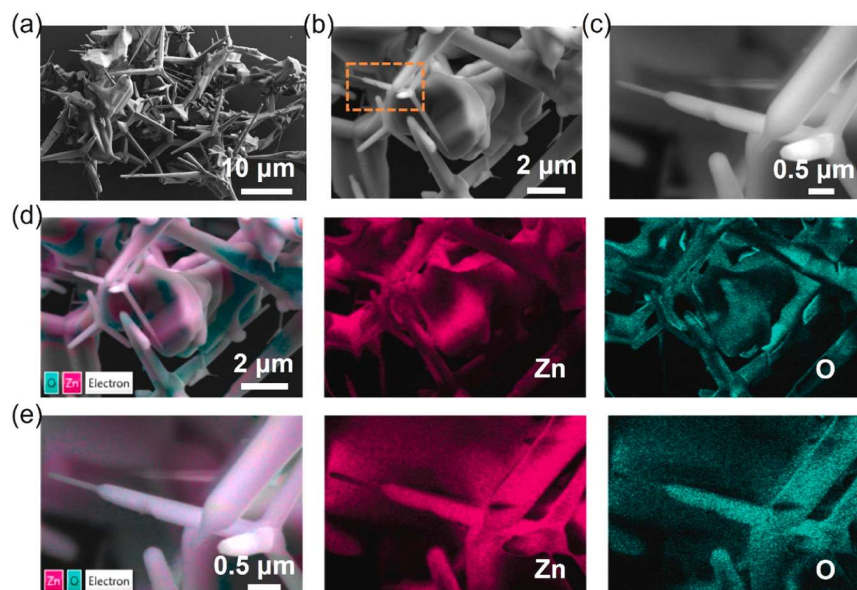


Fig. 2. Morphological and compositional characterization of needle-shaped ZnO structures. (a) Large-scale spatial architecture formed by needle-shaped ZnO. (b) Magnified view of the contact interface within the needle-shaped ZnO structure. (c) Nanoscale junctions formed at needle-shaped ZnO contacts. (d) Elemental distribution of the needle-shaped ZnO structure. (e) Elemental mapping of the junctions formed at needle-shaped ZnO contacts.

further reveals that some ZnO nanoneedles interweave into a three-dimensional network, facilitating gas diffusion and enhancing charge transport pathways, thereby improving NO sensing performance. The high aspect ratio and abundant surface area promote increased NO adsorption, leading to enhanced sensor sensitivity and faster response times (Fig. 2b). Additionally, the nanostructured arrangement enables the formation of efficient contact junctions, which reduce interfacial resistance and stabilize electron transport across multiple conductive pathways (Fig. 2c). Compared to bulk or particulate ZnO, the needle-like architecture provides a more interconnected and continuous electron transport network, further boosting sensor performance. Next, powder X-ray diffraction of the needle-shaped ZnO exhibits the signature reflections at $2\theta \approx 31.7^\circ$ (100), 34.4° (002), 36.2° (101), 47.5° (102), 56.6° (110), 62.8° (103), 66.4° (200), 68.0° (112), and 69.1° (201). The absence of any additional peaks indicates phase-pure and well-crystallized needle-shaped ZnO without detectable secondary phases [35,36] (Fig. S1). Moreover, Fig. S2 shows X-ray photoelectron spectroscopy (XPS) of the needle-shaped ZnO sensing layer. The Zn 2p peaks at 1021.7 eV ($2p_{3/2}$) and 1044.8 eV ($2p_{1/2}$) with 23.1 eV splitting confirm Zn^{2+} in ZnO. In O 1s, the main peak at 529.8 eV arises from lattice oxygen, while the shoulder at ~ 531.2 eV is attributed to vacancy-/OH species ($\text{O}_V/\text{-OH}$). Thus, the surface comprises crystalline Zn–O domains and defect-rich, hydroxylated regions. These $\text{O}_V/\text{-OH}$ sites promote NO adsorption and activation, forming chemisorbed $\text{NO}^-/\text{NO}_2^-$ that withdraw electrons, widen the depletion layer, and increase resistance.

Beyond electrical properties, the mechanical fragility of ZnO presents a challenge for ultraflexible sensor. However, the contact junctions of needle-like ZnO inherently enhances mechanical resilience, mitigating fracture under external stress. These nanostructures maintain stable interfacial contacts during bending, stretching, or compression, thereby preserving electrical functionality under dynamic conditions. Energy-dispersive X-ray spectroscopy (EDS) analysis confirms the uniform elemental distribution of Zn and O within the ZnO nanoneedles, indicating compositional homogeneity (Figs. 2d and 2e). Additionally,

EDS mapping confirms the spatial distribution of ZnO nanoneedles across the sensing layer, aligning with SEM morphology observations and further validating the material's structural and compositional integrity. Thus, SEM characterization provides critical insights into the morphology and growth dynamics of ZnO needles for optimizing their structural properties to enhance NO sensor performance.

3.2. Sensing performance of needle-shaped ZnO resistive sensor

The gas adsorption, desorption, and surface reaction dynamics of ZnO-based materials are strongly temperature-dependent. To elucidate this effect, we evaluated the response of needle-like ZnO and dense ZnO to 5 ppm NO gas across varying temperatures. As shown in Fig. 3a, both materials exhibit a characteristic "increase-peak-decrease" response trend with rising temperature, consistent with prior studies. This behavior arises from the temperature-dependent interplay between adsorption and desorption kinetics. Below 300°C , elevated temperatures enhance the reaction between NO molecules and surface-adsorbed oxygen species, increasing the sensor response. However, beyond this threshold, the accelerated desorption of O_2 and NO from the sensing layer suppresses redox reactions, reducing the response. An optimal balance between these competing processes is achieved at approximately 200°C , where the maximum response is observed. Subsequent experiments were conducted at this optimized temperature to ensure peak sensor performance. Notably, the response value ($S = 59.4$) of the needle-like ZnO sensor is 2.79 times higher than that of dense ZnO ($S = 21.3$), where S is calculated using the formula of $S = R_1/R_0$, with R_0 is initial resistance and R_1 is exposed resistance. This enhanced response is primarily attributed to the needle-like ZnO's larger surface area and higher density of active sites, which promote gas-surface interactions. Additionally, its elongated morphology and sharp-tip junctions facilitate charge carrier accumulation and transport, further improving sensing performance. The dynamic response-recovery characteristics at 200°C , depicted in Fig. 3b, reveal that the needle-like ZnO sensor achieves response and recovery times of 46.5 s and 27.8 s, respectively, upon

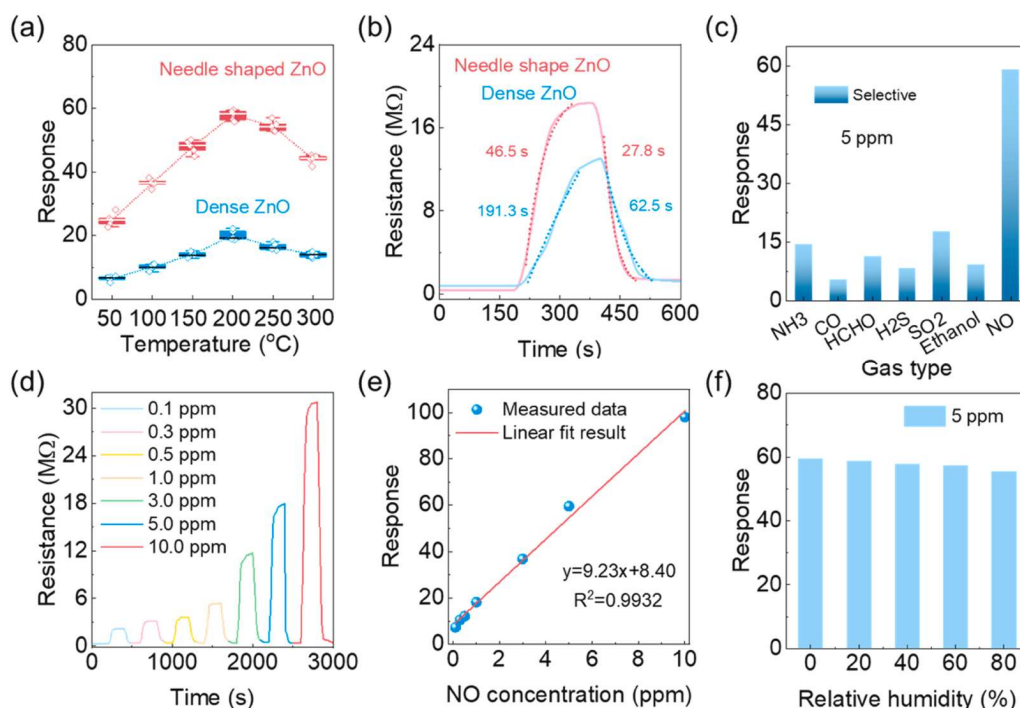


Fig. 3. Sensing performance of the NO sensor. (a) Temperature-dependent curves of NO sensors with dense and needle-shaped ZnO. (b) Temporal response curves of NO sensors with dense and needle-shaped ZnO. (c) Selectivity of the NO sensor based on needle-shaped ZnO. (d) Recovery characteristics of the needle-shaped ZnO sensor at varying NO concentrations. (e) Response of the needle-shaped ZnO sensor to different NO concentrations. (f) Response of the needle-shaped ZnO sensor under varying humidity conditions.

reaching adsorption-desorption equilibrium.

Given the practical advantages of the aforementioned sensor for real-world applications, subsequent experiments focused on the detailed investigation of the sensing performance of the needle-like ZnO material-based sensor. Selectivity is a critical parameter of chemoresistive gas sensors, as it mitigates signal interference in complex environments. To evaluate this, we examined the sensor's response to a range of common volatile organic compounds and inorganic gases, including NH_3 , CO , HCHO , H_2S , SO_2 and Ethanol (Fig. 3c). The sensor exhibited response values between 5 and 15 for these gases, markedly lower than its response to 5 ppm NO ($S = 59.4$), highlighting its superior selectivity for NO detection. In addition, as illustrated in Fig. 3d, exposure of the sensor to an NO -containing atmosphere resulted in a sharp increase in resistance. Upon removal of NO and re-exposure to ambient air, the resistance rapidly reverted to its baseline value. This cyclic response remained highly consistent over multiple repetitions, underscoring the sensor's excellent stability and reversibility. The observed resistance variations align with the established response mechanism of n-type semiconductor sensors to oxidative gases. Specifically, the needle-like ZnO sensor exhibited a pronounced increase in response with rising NO concentrations, suggesting that at higher concentrations, a greater number of NO molecules are rapidly adsorbed onto the sensing layer, where they undergo redox interactions with surface-adsorbed oxygen species, thereby enhancing the sensor's sensitivity. Notably, the sensor displayed a well-defined linear correlation between response and NO concentration over the range of 100 ppb to 10 ppm (Fig. 3e), with a regression equation of $y = 9.23x + 8.40$ and an R^2 value of 0.9932, indicating excellent quantitative reliability. The practical detection limit was determined to be 100 ppb ($S = 1.4$), demonstrating the sensor's capability for trace-level NO detection in environmental monitoring applications. Notably, the sensor maintained similar response retention over 14 days of repeated operation (Fig. S3), underscoring its long-term stability. To assess real-world viability, we further investigated the influence of varying humidity levels (relative humidity: 0 %–80 %) on sensor performance (Fig. 3f). Although the response exhibited a slight attenuation under high-humidity conditions, the sensor's detection capability remained largely unaffected, highlighting its robustness against environmental fluctuations. We also compared our sensor performance with previously reported NO sensors, as indicated in Table S1. It demonstrates higher sensitivity, a lower detection limit, and faster response/recovery dynamics compared with most reported NO sensors. More importantly, our sensor achieves excellent mechanical flexibility, which is rarely realized in conventional inorganic sensors. Therefore, these findings establish the needle-like ZnO-based NO sensor as a highly responsive, rapidly recovering, and exceptionally sensitive platform with stable operation even in humid conditions, making it well suited for real-time NO gas detection and

environmental monitoring applications.

3.3. Ultraflexible needle-shaped ZnO resistive sensors

In flexible electronic applications, sensors are often subjected to varying degrees of mechanical deformations. To evaluate the electrical stability of ZnO-based sensors under such conditions, we systematically investigated the resistance variations of needle-shaped ZnO and dense ZnO sensors under different bending radii (10 mm, 8 mm, 6 mm, 4 mm, 2 mm, and 1 mm), as illustrated in Fig. 4a, the baseline resistance change ratio ($\Delta R/R_0$) was recorded for each case. For dense ZnO, the resistance increased significantly as the bending radius decreased, with a sharp sacrifice of response. In contrast, the needle-shaped ZnO structure exhibited significantly lower resistance variation, with only a slight impact on response even under extreme bending at a 1 mm radius, indicating superior electrical stability. The distinct mechanical responses of these two structures can be attributed to their morphological differences. The densely packed structure of dense ZnO promotes localized stress concentration under bending, facilitating crack propagation and resulting in the breakdown of conductive pathways. Conversely, the needle-shaped ZnO architecture provides multiple contact junctions between nanoneedles, which help maintain electrical connectivity even under deformation, as discussed in morphology section. This structure allows for slight structural reconfiguration, including sliding and realignment of nanoneedles, effectively mitigating stress concentration and minimizing mechanical damage.

To further evaluate the long-term mechanical durability of these sensors, we conducted cyclic bending tests at radii of 8 mm, 4 mm, and 1 mm, systematically monitoring the resistance response over 100, 200, 300, 400, and 500 bending cycles (Figs. 4b and 4c). The dense ZnO sensor exhibited a significant deterioration in performance, retaining only 13.7 % of its initial response after 500 cycles, indicative of severe structural degradation and the eventual failure of the device. In contrast, the needle-shaped ZnO sensor demonstrated exceptional mechanical robustness, with response variations remaining within 20 % even after 500 cycles, underscoring its ability to sustain prolonged dynamic deformation with minimal electrical degradation. These results highlight the critical role of the needle-shaped ZnO architecture in enhancing sensor flexibility and durability while preserving both electrical stability and gas-sensing functionality. The superior mechanical resilience of this structure establishes a strong foundation for the development of next-generation high-performance flexible electronic devices capable of maintaining reliable operation under mechanically demanding conditions.

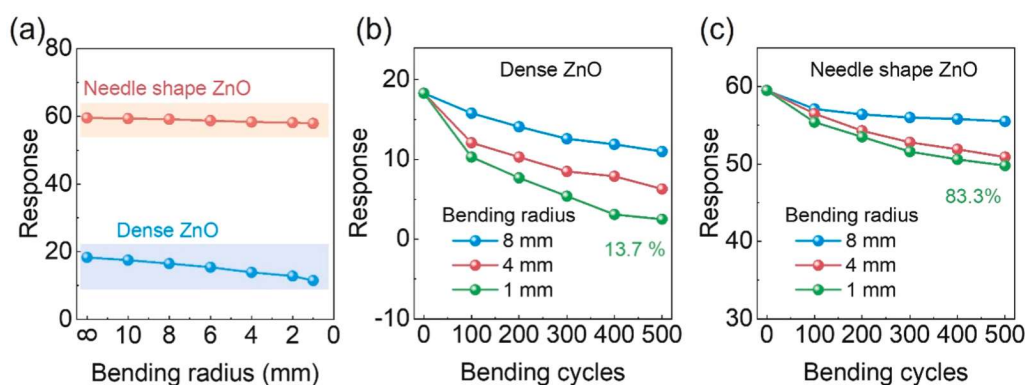


Fig. 4. Performance evaluation of the ultraflexible NO sensor. (a) Response characteristics of NO sensors with dense and needle-shaped ZnO under varying bending radius. (b) Stability assessment of NO sensors with dense ZnO over multiple bending cycles at different radii. (c) Stability assessment of NO sensors with needle-shaped ZnO over multiple bending cycles at different radii.

4. Conclusion

In summary, we have developed an ultraflexible chemoresistive NO sensor based on a needle-shaped ZnO nanostructure, which achieves a remarkable balance between high sensitivity, mechanical durability, and stable operation under dynamic deformation. The unique nanostructured morphology enhances gas adsorption efficiency while enabling robust electrical contact through multiple nanoscale conductive pathways, ensuring reliable performance even under extreme bending conditions. Compared to conventional dense ZnO films, our sensor exhibits significantly enhanced sensitivity ($S = 59.4$), rapid response (<50 s), and excellent selectivity against common interfering gases, while also maintaining stable functionality in high-humidity environments ($>80\%$ RH). Furthermore, the sensor demonstrates outstanding mechanical resilience, retaining its electrical performance after 500 bending cycles at radii as small as 1 mm, underscoring its suitability for real-world applications. The combination of high-performance gas detection and exceptional mechanical flexibility paves the way for future advancements in flexible sensing technologies, offering new opportunities for intelligent bioelectronics and portable environmental diagnostics.

CRedit authorship contribution statement

Jing Xu: Methodology, Investigation, Formal analysis. **Haiting Xu:** Methodology, Investigation, Formal analysis. **Tao Zhang:** Methodology, Investigation, Formal analysis. **Chunying Ou:** Methodology, Investigation, Formal analysis. **Yipeng Pang:** Formal analysis, Data curation, Conceptualization. **Yang Zhang:** Writing – original draft, Formal analysis, Data curation, Conceptualization. **Ding manhua:** Writing – review & editing, Supervision, Funding acquisition, Data curation, Conceptualization. **Li Yang:** Validation, Supervision, Investigation, Funding acquisition.

Declaration of Competing Interest

We declare that we have no financial and personal relationships with other people or organizations that can inappropriately influence our work, there is no professional or other personal interest of any nature or kind in any product, service and/or company that could be construed as influencing the position presented in, or the review of, the manuscript entitled.

Acknowledgement

This work was supported by the General Project of Traditional Chinese Medicine Science and Technology Development Plan in Jiangsu Province (No. MS2023077), the New Round of Xuzhou “Pengcheng Talent Program”-High-level Healthcare Talent Recruitment and Development Project (No. 2025GG005), the Development Fund of Affiliated Hospital of Xuzhou Medical University (No. XYFM202410), the Basic Research Projects of Xuzhou Science and Technology Bureau (No. KC23066) and the Youth Project of Xuzhou Municipal Health Commission (No. XWKYSL20220361).

Appendix A. Supporting information

Supplementary data associated with this article can be found in the online version at [doi:10.1016/j.mtcomm.2025.114358](https://doi.org/10.1016/j.mtcomm.2025.114358).

Data availability

Data will be made available on request.

References

- [1] M.J. Joyner, N.M. Dietz, Nitric oxide and vasodilation in human limbs, *J. Appl. Physiol.* 83 (6) (1997) 1785–1796.
- [2] X. Lu, G.S. Kassab, Integrins mediate mechanical compression-induced endothelium-dependent vasodilation through endothelial nitric oxide pathway, *J. Gen. Physiol.* 146 (3) (2015) 221–232.
- [3] Y. Zhao, P.M. Vanhoutte, S.W. Leung, Vascular nitric oxide: beyond eNOS, *J. Pharmacol. Sci.* 129 (2) (2015) 83–94.
- [4] R. Stanzione, M. Cotugno, F. Bianchi, S. Marchitti, M. Forte, M. Volpe, S. Rubattu, Pathogenesis of ischemic stroke: role of epigenetic mechanisms, *Genes* 11 (1) (2020) 89.
- [5] S. Jackson, A. ElAli, D. Virgintino, M.R. Gilbert, Blood-brain barrier pericyte importance in malignant gliomas: what we can learn from stroke and Alzheimer's disease, *NeuroOncology* 19 (9) (2017) 1173–1182.
- [6] M.K. Ghosh, D. Chakraborty, S. Sarkar, A. Bhowmik, M. Basu, The interrelationship between cerebral ischemic stroke and glioma: a comprehensive study of recent reports, *Signal Transduct. Target. Ther.* 4 (1) (2019) 42.
- [7] E. Bouhamida, G. Morciano, M. Perrone, A.E. Khasay, M. Della Sala, M. R. Wieckowski, F. Fiorica, P. Pinton, C. Giorgi, S. Patergnani, The interplay of hypoxia signaling on mitochondrial dysfunction and inflammation in cardiovascular diseases and cancer: from molecular mechanisms to therapeutic approaches, *Biology* 11 (2) (2022) 300.
- [8] P. Montuschi, M. Santonico, C. Mondino, G. Pennazza, G. Mantini, E. Martinelli, R. Capuano, G. Ciabattini, R. Paolesse, C. Di Natale, Diagnostic performance of an electronic nose, fractional exhaled nitric oxide, and lung function testing in asthma, *Chest* 137 (4) (2010) 790–796.
- [9] S.S. Shetty, D. Deepthi, S. Harshitha, S. Sonkusare, P.B. Naik, H. Madhyastha, Environmental pollutants and their effects on human health, *Heliyon* 9 (9) (2023).
- [10] S.H. Ramalho, A.M. Shah, Lung function and cardiovascular disease: a link, *Trends Cardiovasc. Med.* 31 (2) (2021) 93–98.
- [11] H.M. Tran, F.-J. Tsai, Y.-L. Lee, J.-H. Chang, L.-T. Chang, T.-Y. Chang, K.F. Chung, H.-P. Kuo, K.-Y. Lee, K.-J. Chuang, The impact of air pollution on respiratory diseases in an era of climate change: a review of the current evidence, *Sci. Total Environ.* 898 (2023) 166340.
- [12] N. Zhao, F. Wu, J. Peng, Y. Zheng, H. Tian, H. Yang, Z. Deng, Z. Wang, H. Li, X. Wen, Preserved ratio impaired spirometry is associated with small airway dysfunction and reduced total lung capacity, *Respir. Res.* 23 (1) (2022) 298.
- [13] P. Sedyaw, S. Kawade, D.R. Bhaladhare, K. Pranal, A. Pandey, Causes, effects and management measures of acid rain: a review, *Bhartiya Krishi Anusandhan Patrika* 39 (3) (2024) 215–222.
- [14] G. Richard, W.E. Sawyer, A. Sharipov, Environmental impacts of air pollution. Sustainable Strategies for Air Pollution Mitigation: Development, Economics, and Technologies, Springer, 2024, pp. 47–76.
- [15] S. Pu, Y. Pan, L. Zhang, Y. Lv, Recent advances in chemiluminescence and cataluminescence for the detection of volatile sulfur compounds, *Appl. Spectrosc. Rev.* 58 (6) (2023) 401–427.
- [16] J. Li, A. LoBue, S.K. Heuser, M.M. Cortese-Krott, Determination of nitric oxide and its metabolites in Biological tissues using ozone-based chemiluminescence detection: a state-of-the-art review, *Antioxidants* 13 (2) (2024) 179.
- [17] T.-T. Hung, M.-H. Chung, J.-J. Chiu, M.-W. Yang, T.-N. Tien, C.-Y. Shen, Poly (4-styrenesulfonic acid) doped polypyrrole/tungsten oxide/reduced graphene oxide nanocomposite films based surface acoustic wave sensors for NO sensing behavior, *Org. Electron.* 88 (2021) 106006.
- [18] M. Jiang, C. Wang, X. Zhang, C. Cai, Z. Ma, J. Chen, T. Xie, X. Huang, D. Chen, A cellular nitric oxide sensor based on porous hollow fiber with flow-through configuration, *Biosens. Bioelectron.* 191 (2021) 113442.
- [19] L. Chen, Q. Yu, C. Pan, Y. Song, H. Dong, X. Xie, Y. Li, J. Liu, D. Wang, X. Chen, Chemiresistive gas sensors based on electrospun semiconductor metal oxides: a review, *Talanta* 246 (2022) 123527.
- [20] B. Soltabayev, I.K. Er, H. Surel, A. Coşkun, M.A. Yıldırım, A. Ateş, S. Acar, Influence of Ni doping on the nitric oxide gas sensing properties of Zn1–xNi_xO thin films synthesized by silar method, *Mater. Res. Express* 6 (8) (2019) 086419.
- [21] B. Soltabayev, Y. Raiymbekov, A. Nuftolla, A. Turlybekuly, G. Yergaliuly, A. Mentbayeva, Sensitivity enhancement of CO₂ sensors at room temperature based on the CZO nanorod architecture, *ACS Sens.* 9 (3) (2024) 1227–1238.
- [22] G. Lee, Q. Wei, Y. Zhu, Emerging wearable sensors for plant health monitoring, *Adv. Funct. Mater.* 31 (52) (2021) 2106475.
- [23] R. Kumar, S. Kumar, N. Kalra, S. Sharma, V.E.A. Montaño, A. Singh, Sustainable and facile fabrication of chitosan-coated silver-doped zinc oxide nanocomposites exploiting *Berberis koenigii* foliage for enhanced photocatalysis and antibacterial activity, *Int. J. Biol. Macromol.* 279 (2024) 135162.
- [24] S. Sharma, R. Ponce-Perez, M.G. Moreno-Armenta, J. Guerrero-Sanchez, R. Kumar, S. Kumar, J.M. Siqueiros, O.R. Herrera, An atomic-scale justification for the weak ferromagnetism observed in nanostructured Zn_{0.96-x}Co_xMn_{0.04}O powders, *J. Phys. Chem. C* 128 (28) (2024) 11835–11844.
- [25] M.A. Franco, P.P. Conti, R.S. Andre, D.S. Correa, A review on chemiresistive ZnO gas sensors, *Sens. Actuators Rep.* 4 (2022) 100100.
- [26] C. Li, B.-Y. Song, M.-S. Lv, G.-L. Chen, X.-F. Zhang, Z.-P. Deng, Y.-M. Xu, L.-H. Huo, S. Gao, Highly sensitive and selective nitric oxide sensor based on biomorphic ZnO microtubes with dual-defects assistance at low temperature, *Chem. Eng. J.* 446 (2022) 136846.
- [27] B. Soltabayev, G. Yergaliuly, A. Ajjaq, A. Beldeubayev, S. Acar, Z. Bakenov, A. Mentbayeva, Quick NO gas sensing by Ti-doped flower-rod-like ZnO structures synthesized by the SILAR method, *ACS Appl. Mater. Interfaces* 14 (36) (2022) 41555–41570.

- [28] T. Du, X. Han, X. Yan, J. Shang, Y. Li, J. Song, MXene-based flexible sensors: materials, preparation, and applications, *Adv. Mater. Technol.* 8 (12) (2023) 2202029.
- [29] V.V. Tran, S. Lee, D. Lee, T.-H. Le, Recent developments and implementations of conductive polymer-based flexible devices in sensing applications, *Polymers* 14 (18) (2022) 3730.
- [30] Y. Deng, H. Qi, Y. Ma, S. Liu, M. Zhao, Z. Guo, Y. Jie, R. Zheng, J. Jing, K. Chen, A flexible and highly sensitive organic electrochemical transistor-based biosensor for continuous and wireless nitric oxide detection, *Proc. Natl. Acad. Sci.* 119 (34) (2022) e2208060119.
- [31] B.-Y. Song, C. Li, X.-F. Zhang, R. Gao, X.-L. Cheng, Z.-P. Deng, Y.-M. Xu, L.-H. Huo, S. Gao, A highly sensitive and selective nitric oxide/butanone temperature-dependent sensor based on waste biomass-derived mesoporous SnO₂ hierarchical microtubes, *J. Mater. Chem. A* 10 (27) (2022) 14411–14422.
- [32] D. Klyamer, R. Shutilov, T. Basova, Recent advances in phthalocyanine and porphyrin-based materials as active layers for nitric oxide chemical sensors, *Sensors* 22 (3) (2022) 895.
- [33] D.-W. Jeong, K.H. Kim, B.S. Kim, Y.T. Byun, Characteristics of highly sensitive and selective nitric oxide gas sensors using defect-functionalized single-walled carbon nanotubes at room temperature, *Appl. Surf. Sci.* 550 (2021) 149250.
- [34] B. Almeida, K.E. Rogers, O.K. Nag, J.B. Delehanty, Sensing nitric oxide in cells: historical technologies and future outlook, *ACS Sens.* 6 (5) (2021) 1695–1703.
- [35] R. Gopalakrishnan, M. Ashokkumar, Comparative assessment of transition metals doping effects on structural, optical, optical conductivity, and photocatalytic features of ZnO nanoparticles, *J. Mater. Sci. Mater. Electr.* 35 (24) (2024) 1614.
- [36] P. Ramesh, A. Rajendran, M. Ashokkumar, Biosynthesis of zinc oxide nanoparticles from *Phyllanthus niruri* plant extract for photocatalytic and antioxidant activities, *Int. J. Environ. Anal. Chem.* 104 (7) (2024) 1561–1572.